Gulf General Atomic
Incorporated
P.O. Box 608, San Diego, California 92112

AEC RESEARCH AND
DEVELOPMENT REPORT

GA-9811

GAS-COOLED FAST BREEDER REACTOR

QUARTERLY PROGRESS REPORT

FOR THE PERIOD AUGUST 1, 1969 THROUGH OCTOBER 31, 1969

by

Project Staff

Prepared under
Contract AT(04-3)-167
Project Agreement No. 23
for the
San Francisco Operations Office
U.S. Atomic Energy Commission

Gulf General Atomic Project 393

November 30, 1969

PROGRESS REPORT SERIES

Annual

GA-5537	November 1, 1963 to July 31, 1964
GA-6667	August 1, 1964 to July 31, 1965
GA-7645	August 1, 1965 to July 31, 1966
GA-8107	August 1, 1966 to July 31, 1967
GA-8787	August 1, 1967 to July 31, 1968

Quarterly

GA-8895	August 1, 1968 through October 31, 1968
GA-9229	November 1, 1968 through January 31, 1969
GA-9359	February 1, 1969 through April 30, 1969
GA-9639	May 1, 1969 through July 31, 1969

CONTENTS

FIGURES

FIGURES (Continued)

TABLES

1. INTRODUCTION

Gulf General Atomic Incorporated (GGA) is in its sixth year of work on the Gas-Cooled Fast Breeder Reactor (GCFR) concept under Atomic Energy Commission (AEC) sponsorship. The program effort consists of four tasks: program planning, core design, fuels and materials development, and reactor physics. The broad objectives of the four tasks and the current efforts on each task are summarized below.

1.1. TASK A - PROGRAM PLANNING

Under Task A, a plan for the development and demonstration of the GCFR concept is to be prepared. The planning effort is focused on a detailed definition of the work required to develop a proven core design.

The core development plan that was submitted to the AEC for review is being revised in response to comments and suggestions received from the AEC and from Oak Ridge National Laboratory (ORNL), and a draft of the reactor system development plan has been prepared for submission to the AEC for review.

1.2. TASK B - CORE DESIGN

In this task, detailed analysis of the referenced fuel-rod concept and analysis of alternative core design concepts are to be made. The core design work is concerned with a fuel-rod concept evaluation and the development of an analytical model for the mechanical behavior of the GCFR fuel rods.

During this quarterly period, work continued on the development of the analytical model (BRITL) for the mechanical behavior of the

manifolded-type GCFR fuel rod under irradiation. Creep strains of the cladding and of the fuel are calculated using the viscoelastic approach.

1.3. TASK C - FUELS AND MATERIALS DEVELOPMENT

The objectives of Task C are (1) to review the work from related programs, particularly the Liquid Metal Fast Breeder Reactor (LMFBR) program, that is applicable to the GCFR, and (2) to perform in-pile and out-of-pile tests as part of the overall fuel-element development program for the GCFR.

Surveillance work during this quarterly period was primarily on the effect of fuel-cladding compatibility on fuel-rod behavior. Experiments evaluated were high- and medium-burnup thermal flux tests and fast flux tests.

Fuel irradiation in the Oak Ridge Research Reactor (ORR) is part of a joint Gulf General Atomic - ORNL program in the screening tests of fuel-rod materials and the selection of a fuel-rod concept and design. Postirradiation testing of the three sealed $(Pu-U)O_2$ fuel rods irradiated in an ORR thermal flux to exposures ranging from 47,000 to 59,000 MWd/tonne is continuing. The next phase will be completion of metallographic and burnup analyses. The instrumented manifolded-type $(Pu-U)O_2$ fuel rod for the ORR 04-P9 capsule irradiation test is being encapsulated. Laboratory experiments to determine the diffusion coefficients for the krypton-helium gas pair in the P9 capsule have continued, and work has been initiated to compute the temperature corrections for the thermocouples to be used in the P9 capsule. Startup of the 04-P9 irradiation to the burnup goal of 50,000 MWd/tonne is now scheduled for December 1969.

For the first fast flux irradiations under the GCFR program, a standard B-7 EBR-II subassembly with design modifications is being considered for the irradiation of $(Pu-U)O_2$-fueled GCFR rods. A detailed design analysis was made which established the feasibility of the experiment.

1.4. TASK D - REACTOR PHYSICS PROGRAM

Task D is a cooperative program with Pacific Northwest Laboratory (PNL) to perform experiments in the PNL critical facility. Although the original experimental program has been completed, several additional experiments of interest to the GCFR program are now under way.

Analysis of experiments performed on various 1-to-1 hydrogen-to-plutonium ratio critical assemblies is essentially complete. In addition, three other critical experiments were reevaluated using the current Pu-239 cross-section data of interest. These experiments were the 15-to-1 and 5-to-1 hydrogen-to-plutonium ratio critical assemblies measured at the PNL Critical Mass Laboratory and the Los Alamos JEZEBEL plutonium metal sphere. The results indicate that the Pu-239 data set used gives satisfactory agreement with the experiments over the energy range of the systems.

2. TASK A - PROGRAM PLANNING

The core development plan has been reviewed and revisions are being made in response to comments and suggestions made by the Atomic Energy Commission and Oak Ridge National Laboratory.

A draft of the reactor system development plan has been prepared and will be submitted to the AEC for review and comment. The reactor system has been defined as including the following:

1. Primary coolant system, including main and auxiliary steam generators and coolant circulators

2. Prestressed concrete reactor vessel (PCRV), including all internal structure and penetrations

3. Helium handling and processing system

4. Instrumentation and control system

5. Control rod drives

6. Refueling system

The general format of the plan follows that established for the core development plan.

Preliminary action has been taken to initiate the preparation of the safety development plan, and a tentative list of priorities has been established for the preparation of the remaining program documents.

Programs for the remainder of FY 1970 have been modified to conform to the reduced funding level and to take account of the extension of the contract to the end of FY 1970 instead of until October 31, 1970.

3. TASK B - CORE DESIGN

The title of this task has been changed from "Core Development" to "Core Design" by direction of the AEC; hence, work formerly included in Task B on surveillance of relevant LMFBR fuel work is covered in Task C. The core design work has been curtailed to allow the continuation of the high-priority subtasks in Task C.

3.1. FUEL-ROD CONCEPT EVALUATION

No additional work was done during this period. In previous reports (Refs. 1,2)* the main fuel-rod concepts were discussed and recommendations were made for the selection of a reference fuel-rod concept and an alternative, or backup, concept. The manifolded fuel rod was selected as the reference concept for further detailed GCFR system study and experimental work. The fuel-cladding-interacting fuel rod, which employs a relatively strong cladding as a sealed rod, was selected as the alternative.

3.2. FUEL-ROD BEHAVIOR MODEL

The analytical model (BRITL) of the mechanical behavior of the GCFR fuel element presently in use at GGA considers the interaction of a swelling fuel with a metallic cladding. Creep strains of the cladding and of the fuel considered to be cracked radially due to thermal stresses are calculated using a viscoelastic approach; the radial cracks in the fuel are allowed to close as a result of subsequent swelling and creep.

The main problem is attaining the proper material properties. A review of the data on fuel swelling, fuel creep, cladding creep, and cumulative exhaustion of cladding ductility as subroutines to the main program is being continued.

*References are listed at the end of the section.

REFERENCES

1. "Gas-Cooled Fast Breeder Reactor, Quarterly Progress Report for the Quarters August 1, 1967 to July 31, 1968," USAEC Report GA-8787, Gulf General Atomic, September 1968.
2. "Gas-Cooled Fast Breeder Reactor, Quarterly Progress Report for the Period August 1 through October 31, 1968," USAEC Report GA-8895, Gulf General Atomic, December 1968.

4. TASK C - FUELS AND MATERIALS DEVELOPMENT

4.1. THE EFFECT OF FUEL-CLADDING COMPATIBILITY ON FUEL-ROD BEHAVIOR

Fuel-fission product-cladding reactions may limit the fast reactor fuel-rod operating temperature and life and, in addition, are a factor in determining the cladding thickness required. Surveillance relative to these reactions is an essential part of the GCFR review of LMFBR fuel work.

No cladding failures occurred in the high-burnup thermal flux tests, even though significant amounts of fuel-cladding chemical interactions were observed (Ref. 1). In rods irradiated to 136,000 MWd/tonne, with 347 stainless-steel-cladding inner surface temperatures ranging from 650 to 760 C, 0.003 to 0.005 in. of cladding reacted in areas where the calculated cladding temperature was 700 to 760 C. However, the interaction was generally less than 0.001 in., with localized reaction up to 0.002 in. in a section where the cladding had operated at 650 C (Ref. 1).

Stratification of iron, nickel, and chromium was revealed by electron microprobe analysis, and iron was found combined with metallic fission products through the equiaxed fuel structure and as free iron in the reaction zone. Chromium was combined with fission products in the reaction zone. Palladium, molybdenum, barium, and cesium were also found in the fuel-cladding reaction zone. The highest concentrations of these fission products were adjacent to the cladding, but none were detected in the cladding matrix or grain boundaries. Islands of fuel were also found in the fuel-cladding reaction zone.

In another GE thermal flux experiment (Refs. 2,3), in which $(Pu\text{-}U)O_2$ fuel (O/M = 2.00) clad with 347 stainless steel was exposed to medium burnup of 45,000 MWd/tonne, slight to moderate fuel-cladding reactions below 650 C and significant to severe reactions above 650 C were exhibited. The reactions extended to a depth of 9 mils at 720 C, which is an unacceptable amount for any fuel-rod design contemplated.

The rod failed after approximately 1000 hr of operation but was irradiated for an additional period of approximately 2000 hr after the failure. It is not known to what extent the presence of NaK in contact with the fuel and cladding during this 2000-hr period influenced the fuel-cladding interaction. The results from this 3000-hr irradiation are in general agreement with other thermal flux irradiations which ran from 6000 to 10,000 hr and in which no failures occurred.

GCFR thermal irradiations of UO_2-fueled and $(Pu\text{-}U)O_2$-fueled rods clad with Hastelloy-X have exhibited fuel-cladding chemical reactions when the cladding surface operating temperatures have been >700 C (Ref. 4). The reactions appear to be more extensive in regions where the fuel is not in contact with the cladding, suggesting that the reaction results from some gaseous material (possibly oxygen or fission products released from the fuel).

In GE fast flux tests of 11 stainless-steel-clad mixed oxide fuel rods irradiated to 50,000 MWd/tonne at cladding i.d. temperatures up to 620 C very little reaction occurred. In one rod, localized cladding thinning of up to 0.002 in. was observed. This rod operated with the highest cladding i.d. temperature of all the rods examined, i.e., 620 C. A reaction zone $\sim$0.001 in. thick was observed adjacent to and around the fuel circumference. Microprobe analysis of the reaction zone indicated a nonuniform distribution of iron, chromium, and nickel across the zone, a decrease in the chromium concentration in the reaction phase near the fuel, a nonuniform but generally decreasing iron content near the fuel, and a nearly constant nickel composition. No plutonium or uranium was found in the reaction

zone, nor were any of the stainless steel alloying elements (iron, nickel, chromium, niobium, tantalum, or manganese) found in the fuel. The presence of other fission products, specifically cesium, in the cladding was not detected by the microprobe.

Chemical analysis of a cladding sample from a second rod indicated that cesium was present in the cladding and that both cesium and tellurium were present in the reaction phase.

In another group of four rods irradiated to 75,000 MWd/tonne at cladding temperatures at or below 600 C, a decrease in cladding thickness of 0.0005 in. was observed. Some localized cracks of unknown origin (0.005 in. deep) were observed in the i.d. of a section from one of the rods (Ref. 1).

The Argonne National Laboratory (ANL) microprobe results on sections of fuel rods irradiated in fast flux tests showed large concentrations of cesium (a daughter product of iodine) in the grain boundaries of 304 stainless steel cladding to a depth of 4 mils, where the fuel-cladding interface operated at ∿600 C. After dry storage of the sample for three months, grain boundary cohesion near the inner surface of the cladding was lost and fission product penetration to a depth of 9.4 mils was detected (Ref. 5). Iron, nickel, manganese, and chromium were also found in (Pu-U)O_2 fuel (Ref. 6). It has been proposed that the iron may be transported by fission-product iodine as FeI_2 by means of a chemical transport reaction (Ref. 7).

4.2. IRRADIATION TEST PROGRAM (IN-PILE AND OUT-OF-PILE TESTS)

4.2.1. Introduction

The GCFR fuel-element development program includes the irradiation testing of fuel rods under GCFR design test conditions, particularly under conditions that are not included in the LFMBR irradiation testing program.

Both thermal and fast flux tests are included in the GCFR program. The thermal flux irradiation program is a joint effort of GGA and ORNL, with the irradiations performed in the ORR poolside facility (Ref. 8). Data from the irradiations will be used to select the most promising fuel-rod design features and parameters to be incorporated in future loop irradiations and fast flux capsule tests. Design of a fast flux (EBR-II) capsule B-7 subassembly test is currently under way. Data on irradiation tests to date, tests under way, and tests being planned are summarized in Table 4.1.

4.2.2. 04-P8 Irradiation Capsule

Postirradiation examination of the three sealed (Pu-U)O_2-fueled rods that were irradiated in capsule 04-P8 (Ref. 9) to burnups ranging from 47,000 MWd/tonne to 59,000 MWd/tonne, at linear power ratings from 13 to 15.5 kW/ft, and at cladding o.d. temperatures from 610 to 685 C is continuing at ORNL. During this period the fuel rods were sectioned for metallography and burnup analysis. Visual examination of the sections revealed no unusual or unexpected changes in the fuel. The central hole of the annular pellets was shifted ∿7% to 8% off-center in the hottest axial positions, and only slight variations (not yet measured) in the size of the central hole were observed.

During this period, metallographic examination of sections from the rods was begun. The fuel (mechanically blended 88 wt-% UO_2 - 12 wt-% PuO_2) structure in each of the rods was normal for operation at the heat ratings from 13 to 15.5 kW/ft (see Fig. 4.1). Near the fuel o.d., discreet particles of PuO_2 were uniformly distributed among UO_2 particles, and it was apparent that the PuO_2 particles had operated at a higher temperature than the UO_2 particles. The PuO_2 particles contained large "bubbles" distinguishable from the as-fabricated pores. In the equiaxed grain growth region (extending to ∿0.7 R) some interdiffusion between UO_2 and PuO_2 had occurred, and in the columnar grain growth region (extending to ∿0.5 R) the fuel appeared to be "solid solution" (Pu-U)O_2. Cesium, in the form of a white crystalline growth and identified by gamma spectroscopy, was found to be distributed predominantly in the cracks in the fuel and near the o.d. and other cooler regions of the fuel.

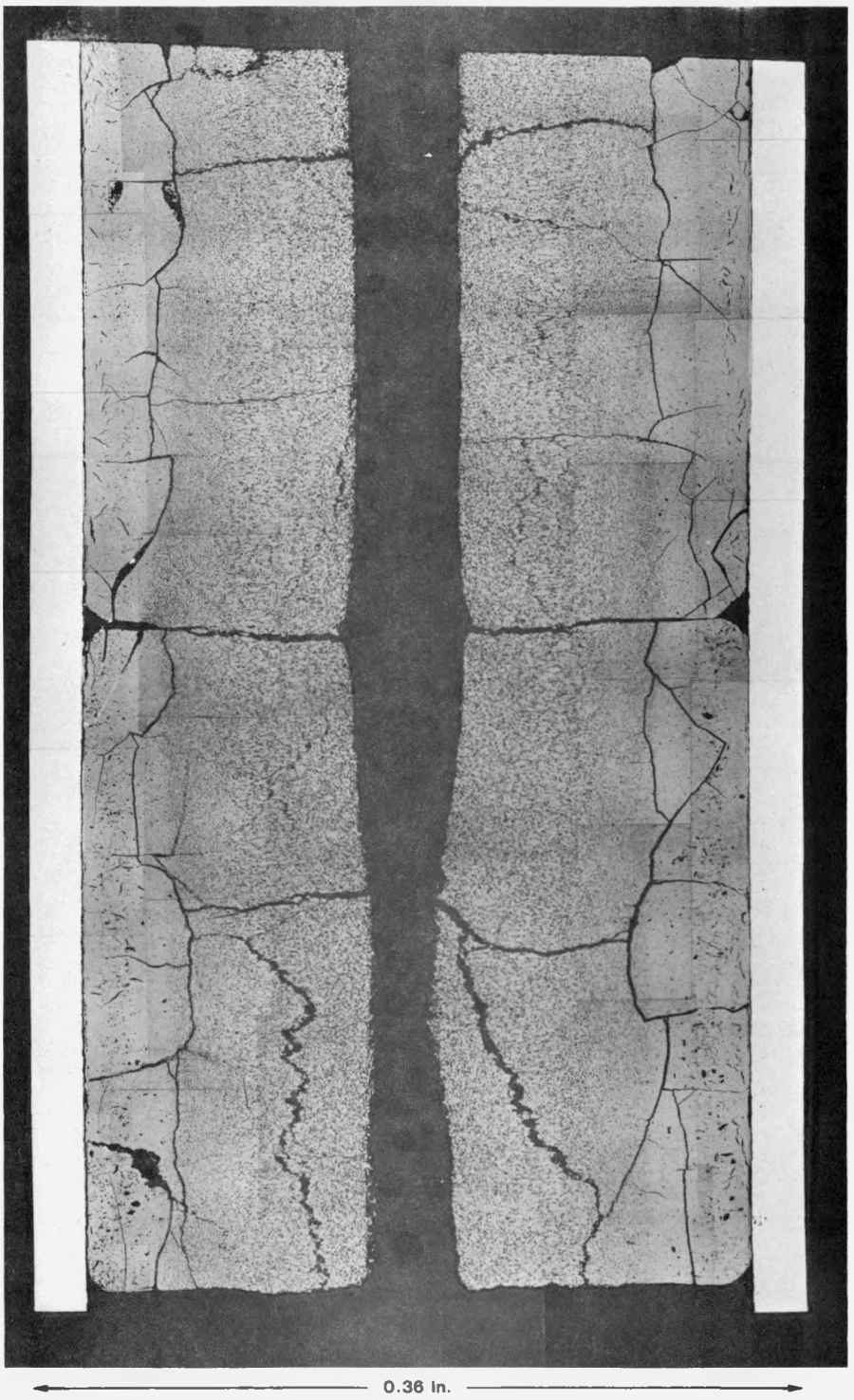

K76579

Fig. 4.1. Fuel structure in specimen GA-17 irradiated in capsule 04-P8. Note that structure is normal for rod irradiated at 13 kW/ft.

TABLE 4.1
SUMMARY OF GCFR IRRADIATIONS

Test Identification	Test Reactor and Position	Schedule of Irrad. (hr)	Fuel-rod Type	Fuel-Clad. Thermal Bond	Fuel: Composition	Fuel: % TD[a]	Fuel: Geometry	Fuel: Stoichiometry (O/M)	Fuel: Fuel-Cladding Gap (in.)	Cladding: Composition	Cladding: Thickness OD (in.)	Conditions: Heat Rating (kW/ft)	Conditions: Max. Cladding Temperature (C)	Conditions: Burnup (MWD/tonne) Heavy Metal	Significant Features or Results
Gulf General Atomic–Oak Ridge National Laboratory GCFR Development-Program Thermal-flux Irradiation Tests Completed															
P4-A1 GA-1	ORR-P4	650	Sealed can	He	UO_2	~90	P,A[b]	2.005	0.0018	Hastelloy-X	0.0091/0.379	18/21.7	760		Specimens collapsed; negl. fuel support
GA-2	ORR-P4	650	Sealed can	He	UO_2	~90	P,A	2.005	0.0028	Hastelloy-X	0.0092/0.378	18/21.7	760	3,400	
P4-B2 GA-4	ORR-P4	800	Sealed can	He	UO_2	~90	P,A	2.006	0.001/0.0025	Hastelloy-X	0.014/0.342	18/16.2	760/673		Good condition; collapse in region of thin cladding; negligible fuel support
GA-5	ORR-P4	800	Sealed can, tapered cladding	He	UO_2	~90	P,A	2.006	0.0008/0.0023	Hastelloy-X	0.010-0.020/ 0.334-0.352	18/16.2	760/565	4,500	
P4-B3 GA-6	ORR-P4	1,340	Flex-can	Na	UO_2	~95	P	2.005	0.017	304 SS	0.010/0.375	14.7	650	5,600	Slight creep deformation
GA-7	ORR-P4	1,340	Sealed can	He	UO_2	~90	P,A	2.003	0.0036	Hastelloy-X	0.015/0.343	12.1	650	5,700	
P4-B4 GA-8	ORR-P4	2,000	Flex-can (c)	Na	UO_2	~95	P	2.0032	0.015	304 SS	0.010/0.375	13.5/15.1	700/715	8,300	Good collapse stability
GA-9	ORR-P4	2,000	Sealed can,PP	He	UO_2	~90	P	2.0032	0.0036	Hastelloy-X	0.015/0.343	11.4/12.6	650/715	8,800	
O4-P5 GA-10	ORR-O4	2,200	Sealed can,PP	He	UO_2	~90	P,A	2.0039	0.0035	Hast.-X partially surface-roughened	0.015/0.343	14.0	710	11,000	Some cladding deformation under thermocouple used to monitor temperature of OD
GA-11	ORR-O4	2,200	Sealed can,PP	He	UO_2	~90	P,A	2.002	0.0035	Hast.-X partially surface-roughened	0.015/0.343	16.2	812	12,000	Good collapse stability
GAL-1 ORR Exp 16	ORR Loop	~4 total	Sealed can	He	UO_2	~90	P,A	2.003	0.003	Hast.-X partially surface-roughened	0.015/0.343	16	812	~10	
O4-P6 GA-12	ORR-O4	1,100	Sealed can	He	88 UO_2–12 PuO_2	~90	P,A	1.98/1.99	0.0033	Hast.-X partially surface-roughened	0.015/0.343	15	710	4,200	Good collapse stability
GA-13	ORR-O4	1,100	Sealed can	He	88 UO_2–12 PuO_2	~90	P,A	1.98/1.99	0.0033	Hast.-X partially surface-roughened	0.015/0.343	18	812	4,800	Collapsed into oval shape; negligible fuel support
GA-14	ORR-O4	1,100	Sealed can,PP	He	88 UO_2–12 PuO_2	~90	P,A	1.98/1.99	0.0033	Hast.-X partially surface-roughened	0.015/0.343	18	838	4,800	Cladding failed under thermocouple band; negligible fuel support
O3-P7 GA-15	ORR-O3	~7,800	Sealed can	He	UO_2	~90	P,A	2.002	0.0025	Hastelloy-X	0.020/0.353	6.8	750	~16,000	Irradiation discontinued at 16,000 MWd/tonne
GA-16	ORR-O3	~7,800	Sealed can	He	88 UO_2–12 PuO_2	~90	P,A	1.98/1.99	0.0034	Hastelloy-X	0.020/0.353	8.2	750	~16,000	Fission-product leak detected in rod
O4-P8 GA-17	ORR-O4	~11,000	Sealed can	He	88 UO_2–12 PuO_2	~90	P,A	1.98/1.99	0.002	316 SS	0.024/0.355	13.2	610[d]	~47,000	
GA-18	ORR-O4	~11,000	Sealed can	He	88 UO_2–12 PuO_2	~90	P,A	1.98/1.99	0.003	Hastelloy-X	0.015/0.343	15.5	700	~59,000	Fuel-rod specimens all in excellent condition; little, if any, deform. observed
GA-19	ORR-O4	~11,000	Sealed can,PP	He	88 UO_2–12 PuO_2	~90	P,A	1.98/1.99	0.003	Hastelloy-X	0.015/0.343	15.5	700	~59,000	
Gulf General Atomic GCFR Development-Program Irradiation Tests Planned															
Thermal-flux Tests[e]															
O4-P9	ORR	~11,000	Manifolded to external plenum	He	88 UO_2–12 PuO_2	~90	P,A	~1.98	~0.003-0.004	316 SS	0.024/0.355	15	700	>50,000	Fission-product emission at top of fuel rod and top of fission-product trap will be monitored; instrumented rod and trap; rod external pressure ~950 psi, internal pressure ~1000 psi under normal operating conditions.
Fast-flux Tests															
F-1 Subassembly (7 rods)	EBR-II	~10,000	Manifolded to ext'nl plenum	He	85 UO_2-15 PuO_2	~90	P, A	~1.98	~0.002-0.003	316 SS	OD/ID ~1.15	12 - 16	600-800	>50,000	Not instrumented; ambient pressure
F-2 Subassembly (7 rods)	EBR-II	~10,000 to 20,000	Manifolded to ext'nl plenum and sealed can	He	85 UO_2-15 PuO_2	~90	P, A V[f]	~1.98	~0.002-0.003	316 SS Hast.-X (sealed can only)	OD/ID ~1.15	12 - 16	700-800	>50,000	Not instrumented, ambient pressure. Some sealed rods with high-strength cladding may also be included.

[a] Smear density was less than or equal to 85% of theoretical.

[b] Pellet, annular.

[c] PP = Prepressurized rod (external pressure 800 to 1000 psi in capsules, 300 psi in loop.

[d] Temperature swing on this rod was from 560 C to 660 C during each reactor cycle.

[e] Irradiation scheduled to start 12-12-69.

[f] Vibratory compacted.

An unidentified material with an "as-cast" structure was found in the axial hole of the lower rod GA-19, at a location in which an unexpected large activity peak (corresponding to the fourth pellet from the top) was detected during gamma scanning. The unidentified material is shown in Fig. 4.2. Microprobe analysis to determine the composition of the material is planned. Fuel swelling in each of the rods apparently was counteracted by sintering and/or was accommodated in the hole in the annular pellets, since no measurable fuel-length change or significant cladding diameter change was in evidence.

A uniform fuel and/or fission product-cladding reaction layer approximately 0.002 in. thick was present in both the 316 stainless-steel-clad upper rod GA-17, which operated at maximum cladding o.d. temperatures from 565 to 665 C, and the Hastelloy-X-clad rods GA-18 and GA-19, which operated at maximum cladding o.d. temperature of 685 C (see Fig. 4.3). The reaction layer was located so that ∿80% of its thickness was in the fuel and the remainder appeared to be in the cladding, but no measurable cladding thickness change was observed. None of the subsurface porosity that has been observed near the cladding inner surface in previous higher temperature (∿800 C) tests was found except for perhaps a localized, barely detectable trace near one pellet/pellet interface in the 316 stainless-steel-clad rod GA-17. Microprobe analysis to identify the reactions observed is planned. No grain growth was observed in the 316 stainless steel cladding, although the grain boundaries near the inner surface were wider than those near the outer surface. This is assumed to have resulted from more carbide precipitation near the inner surface, which operated at a temperature ∿50 C higher than the outer surface. No structural changes were in evidence in the Hastelloy-X cladding.

The results of the postirradiation external visual examination, dimensional measurements, fission gas release measurements, and gamma scanning of the 04-P8 fuel rods were reported previously (Ref. 10). Additional postirradiation examination will include:

1. Burnup analysis and neutron dosimetry wire analysis

2. Microprobe analysis where the requirement is indicated

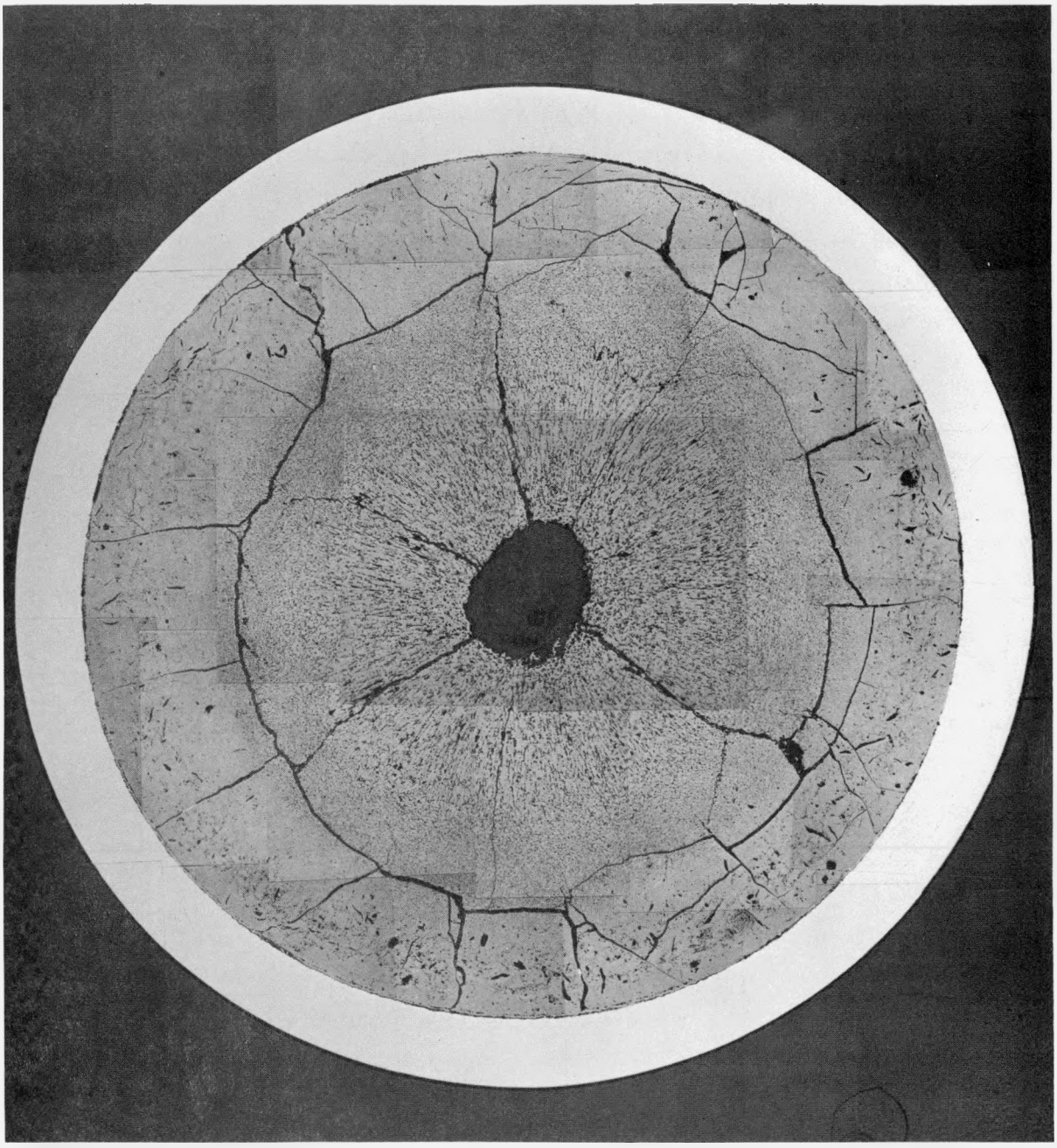

K76580

Fig. 4.2. Illustration of narrow but rather uniform fuel - fission product - cladding reaction layer in specimen GA-17 irradiated in capsule 04-P8

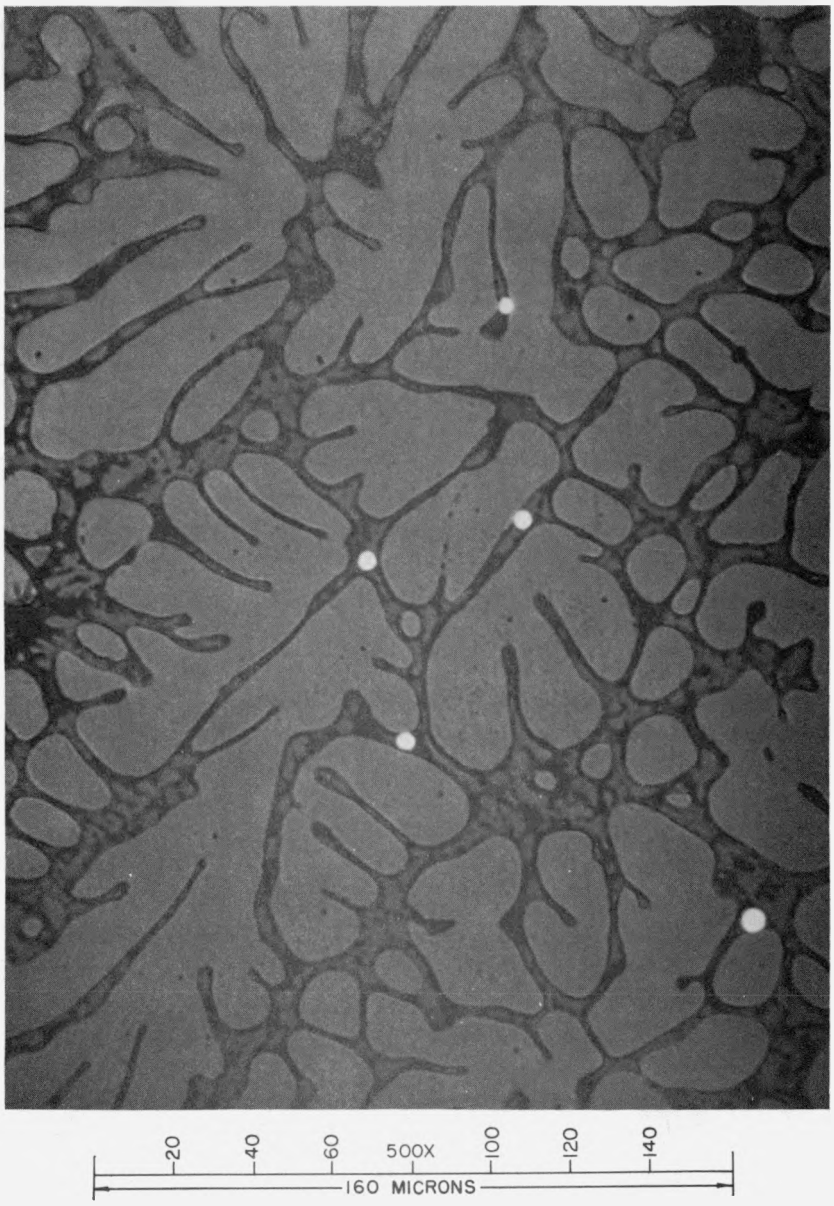

R49894

Fig. 4.3. Illustration of "as-cast" structure in fuel near center of pellet in fuel-rod specimen GA-19 in location at which anomalously high gamma peaking was observed

3. Cladding mechanical property tests to evaluate the amount of degradation associated with fuel-cladding interaction, neutron irradiation, and thermal history

Planned fuel-rod plenum analyses for fission product distributions were deferred and fuel-rod internal void volume measurements were cancelled as a result of program funding limitations.

4.2.3. 04-P9 Irradiation Capsule

Encapsulation of the manifolded-type $(Pu-U)O_2$-fueled rod to be irradiated (scheduled to start December 12, 1969) in capsule 04-P9 at a linear heat generation rating of 15 kW/ft and a cladding o.d. temperature of 700 C to a burnup ≥50,000 MWd/tonne continues at ORNL. The objectives of the irradiation, discussed previously in Ref. 9, include evaluation of the charcoal fission product trap. Preirradiation evaluation accomplished during this period is described in Section 4.2.3.2. The fuel rod will contain a fission product trap that will operate with an outer surface temperature of ∿300 C. The planned test conditions for capsule 04-P9, the design of the fuel-rod specimen and capsule, and the design of the fission product trap monitoring system have been reported previously (Ref. 8).

4.2.3.1. 04-P9 Capsule Temperature Corrections Based on Power Distribution. Work has been initiated to compute the temperature corrections that should be applied to the thermocouples that will be used in capsule P9 to control the test and to control the temperature of the outer cladding surface to a maximum of 700 C. Two factors contribute to the need for corrections: (1) the fuel rod will be located on the reflector flux peak in a steep flux gradient, resulting in asymmetric power generation in the rod; and (2) the thermocouples are separated from the cladding surface by an annulus of NaK and are spaced vertically and circumferentially. Power distribution within the rod has been computed. The power distribution will be used as input to the RAT or TAC programs to compute the radial and circumferential temperature corrections at each vertical location of the thermocouples.

Since these profiles are related to the core loading scheme, it is planned that the calculational effort will be extended if the loadings of the elements adjacent to the capsule are substantially altered in future cycles. The nuclear analysis of the power distribution in capsule P9 is discussed below.

System Geometry

The P9 capsule will be operating in position 04 of the ORR facility, shown in Fig. 4.4. The fuel loading pattern varies from cycle to cycle; however, the fissile weights given in Fig. 4.5 for cycle 87A may be considered typical. Each element also nominally contains 3.926 kg of aluminum and 2.271 kg of H_2O.

The capsule dimensions are listed in Table 4.2. The fuel region consists of 32 mixed oxide pellets [88 wt-% UO_2 (9% enriched) - 12 wt-% PuO_2] with the following plutonium isotopic composition:

Pu-239	90.4 wt-%
Pu-240	8.06 wt-%
Pu-241	0.90 wt-%
Pu-242	0.06 wt-%

The active fuel length of 9.24 in. is separated from the depleted UO_2 blanket by two suppressor pellets with enrichments of 14.9% and 8.3%.

Calculational Procedure and Results

A six-group cross-section set, with the structure given in Table 4.3, was used for all calculations. In the core region, the spectrum was taken to be that of a fresh ORR element; in the capsule region, an infinite water spectrum was assumed. In each case, the leakage was treated in the normal manner, i.e., by adding an axial leakage correction, DB_z^2, to the capture cross section. A 2DF calculation with the geometry shown in Figs. 4.6 and 4.7 then yielded the in-capsule power distribution

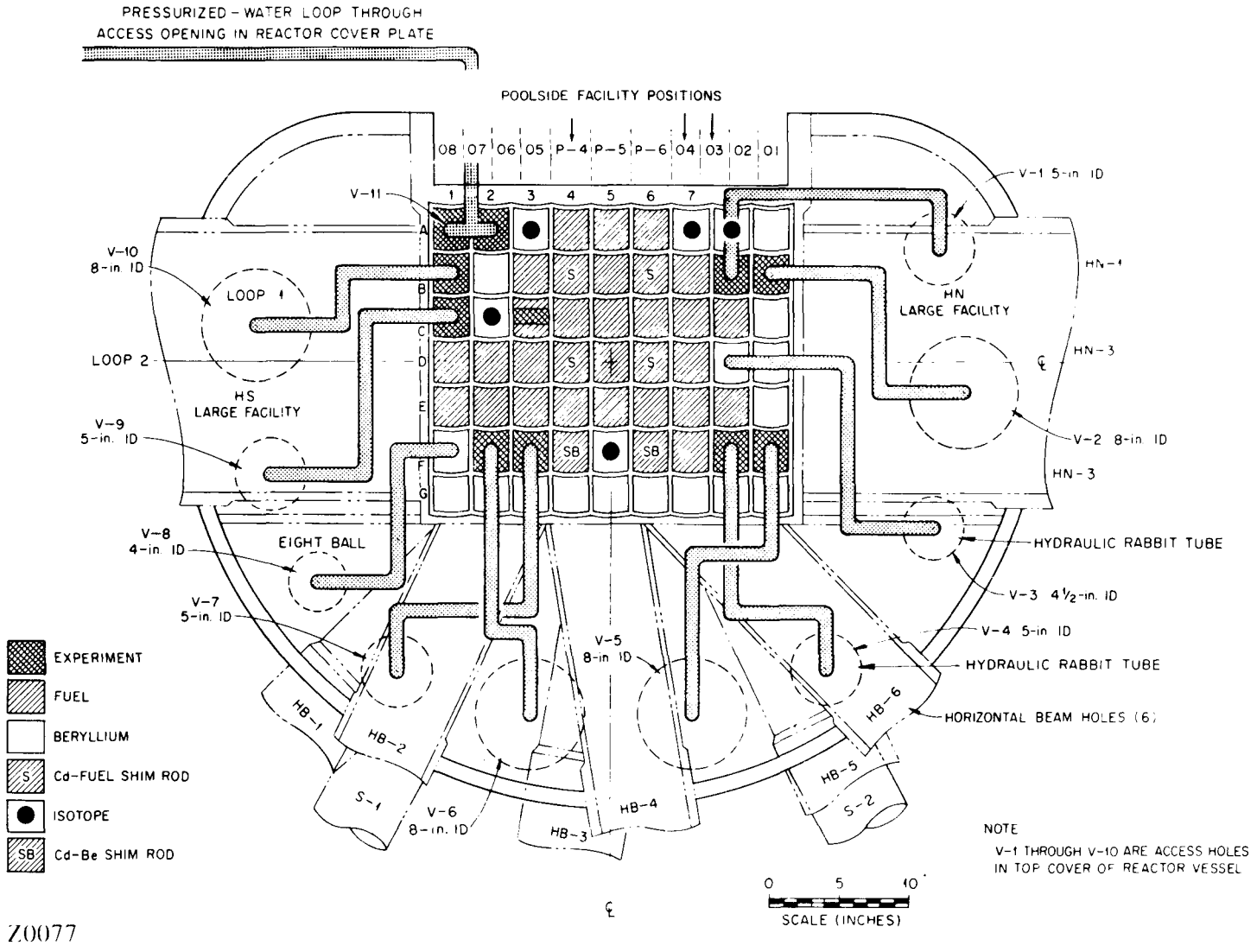

Fig. 4.4. Plan view of ORR showing fuel loading and irradiation facilities location

ORR CORE

CYCLE 87A
START: JUNE 27, 1969
END: JULY 2, 1969

P-5
POOL

MWh: 2538.72
TOTAL U-235: 4982.627

				W				
A-1	A-2	A-3	A-4 47-L 202.30	A-5 84-L 238.24	A-6 58-L 201.97	A-7	A-8	A-9
B-1	B-2	B-3 75-L 239.30	B-4 SR-34 65.740	B-5 9-L 170.90	B-6 SR-35 59.39	B-7 77-L 236.91	B-8	B-9
C-1	C-2	C-3 90-K 137.44	C-4 24-L 135.88	C-5 43-K 132.55	C-6 75-K 135.93	C-7 17-L 138.19	C-8 6-L 172.25	C-9
D-1	D-2	D-3 39-L 198.32	D-4 SR-36 92.675	D-5 92-K 161.44	D-6 SR-37 83.432	D-7 48-L 199.26	D-8	D-9
E-1	E-2	E-3 82-L 242.05	E-4 13-L 175.44	E-5 27-M 126.27	E-6 26-L 176.47	E-7 86-L 238.63	E-8 96-K 161.51	E-9
F-1	F-2	F-3 43-L 193.78	F-4 SR-38 155.39	F-5 97-K 162.06	F-6 SR-39 156.94	F-7 49-L 191.97	F-8	F-9
G-1	G-2	G-3	G-4	G-5	G-6	G-7	G-8	G-9

S

N

E

GANG ROD POSITION AT CRITICAL: 14.780
DOWNTIME FROM SHUTDOWN TO CRITICAL: 123.5 HR

Fig. 4.5. U-235 loadings of ORR for cycle 87A

TABLE 4.2
CAPSULE GEOMETRY

Material	Outer Diam (in.)
Void	0.06
Fuel	0.3007
Void	0.3045
Cladding	0.353
NaK	0.445
Zr	0.740
NaK	0.900
304 SS	1.057
He	1.060
304 SS	1.22

TABLE 4.3
ENERGY GROUP STRUCTURE

Group	Lower Energy (eV)
1	4.98×10^5
2	9.12×10^3
3	2.38
4	0.10
5	0.05
6	0.0

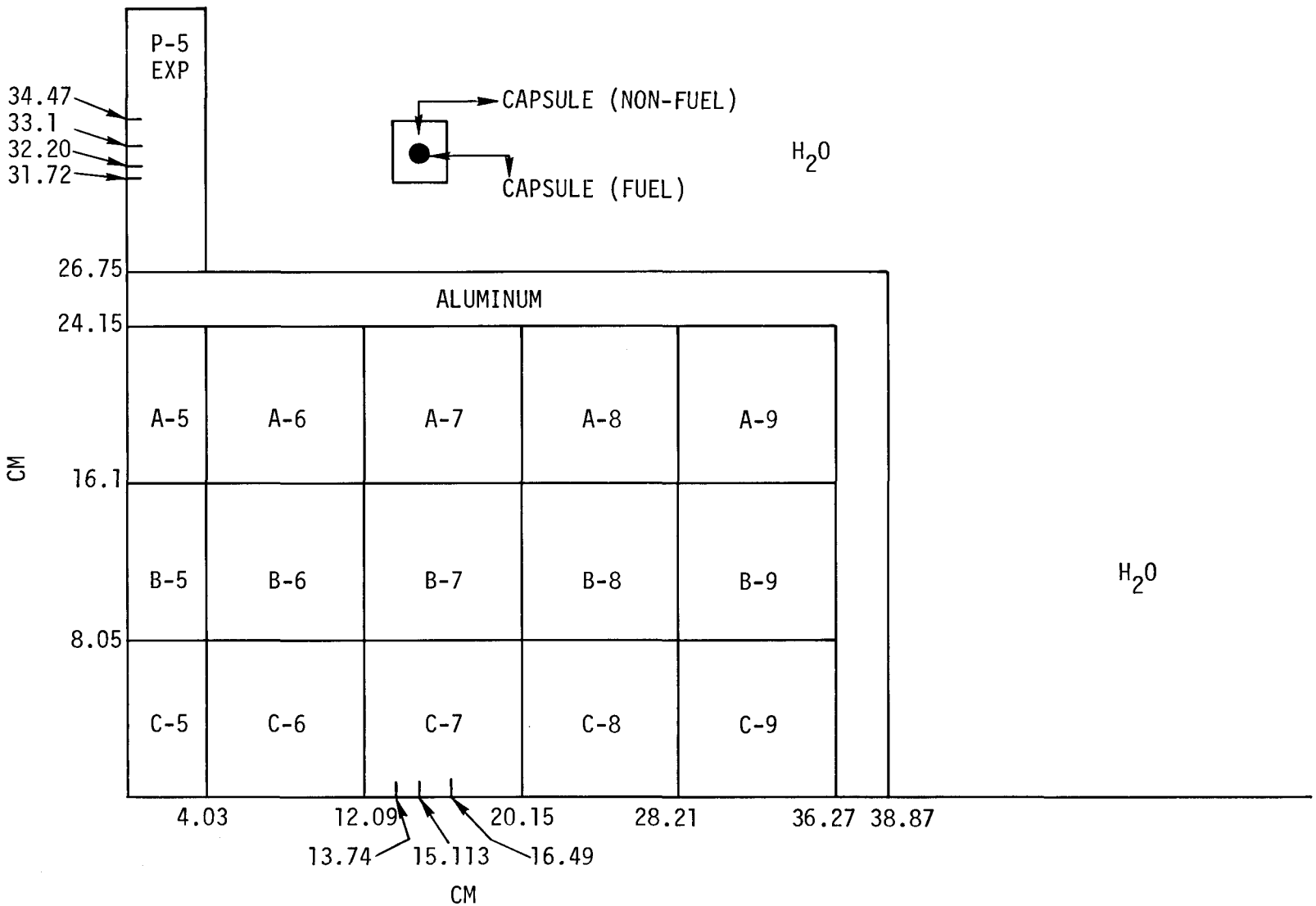

Fig. 4.6. 2DF X-Y geometry

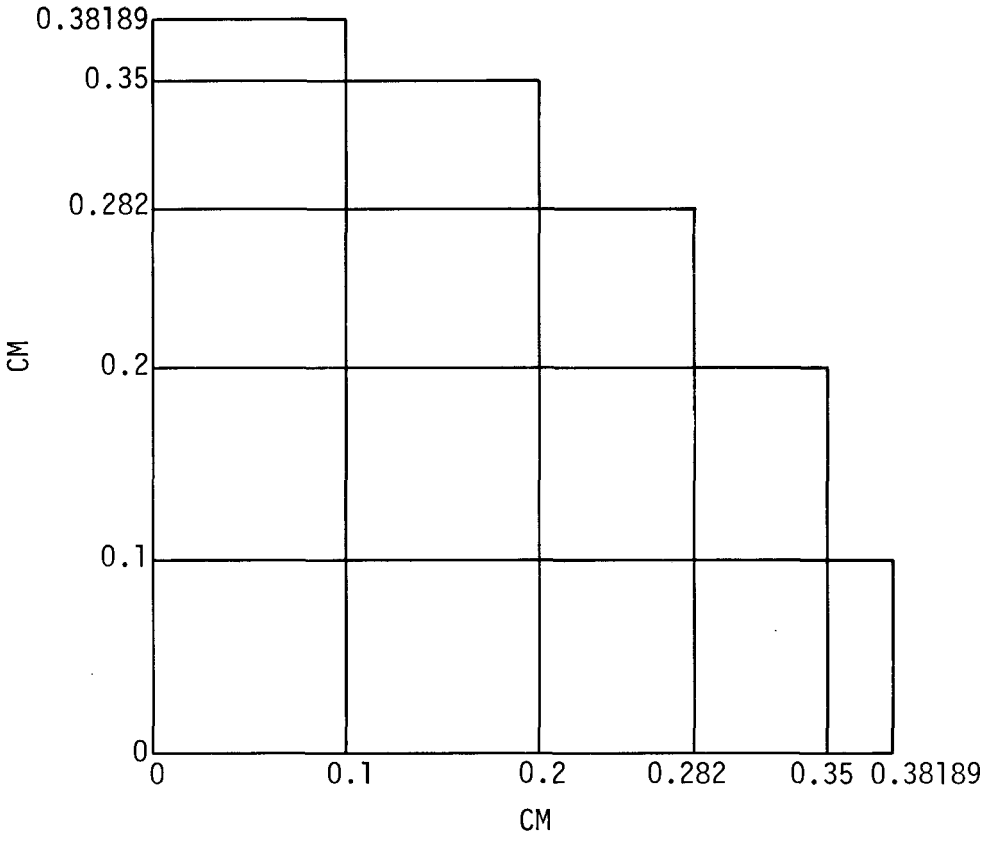

Fig. 4.7. Detailed capsule geometry

of Fig. 4.8. During burnup, the radial power distribution will tend to flatten in an azimuthally asymmetric manner. Methods are available to calculate this behavior precisely; however, the magnitude of the asymmetry (as judged by the success of an approximation for a previous capsule) and the existing uncertainty in core loadings (and hence incident flux distribution) did not appear to justify the extensive effort (∿4 computer hours) required.

Figure 4.9, a plot of the power shift with lifetime, is based on a study performed for a previously irradiated capsule (Ref. 11) of slightly lower enrichment. A calculation at the beginning of life (BOL) demonstrated that increasing the U-235 enrichment to the present value of 9% did not alter the flux shape significantly. It should be noted that the one-dimensional technique used to obtain these results cannot reproduce the two-dimensional values exactly along any radius because it assumes a zero azimuthal gradient.

The axial thermal flux shape at the 05 location was measured in a recent experiment (Ref. 12) and is shown in Fig. 4.10. Since most of the power production is caused by thermal neutron fissions at the capsule edge, the axial power shape at BOL will correspond very closely to this plot. The fueled region will extend from the core bottom to centerline and, consequently, the axial profile will also be given by Fig. 4.10. During the year of full-power operation, the curve will shift because of changes in the source shape due to control-rod motion and core burnup, and it will flatten because of uneven axial burnup.

The axial shift introduces an uncertainty of ∿10% into the predicted flux levels for a quoted shift of ∿2.5 in. The axial flattening was estimated by assuming a constant flux shape and observing the relative flattening along the axis. It was found that, even under this conservative assumption, the peak power was determined by the peak of the incident flux. Consequently, the influence of axially uneven burnup on the planned experiment should be negligible. However, if the main thermocouple should fail, it would be advisable to recalculate the axial distribution for the

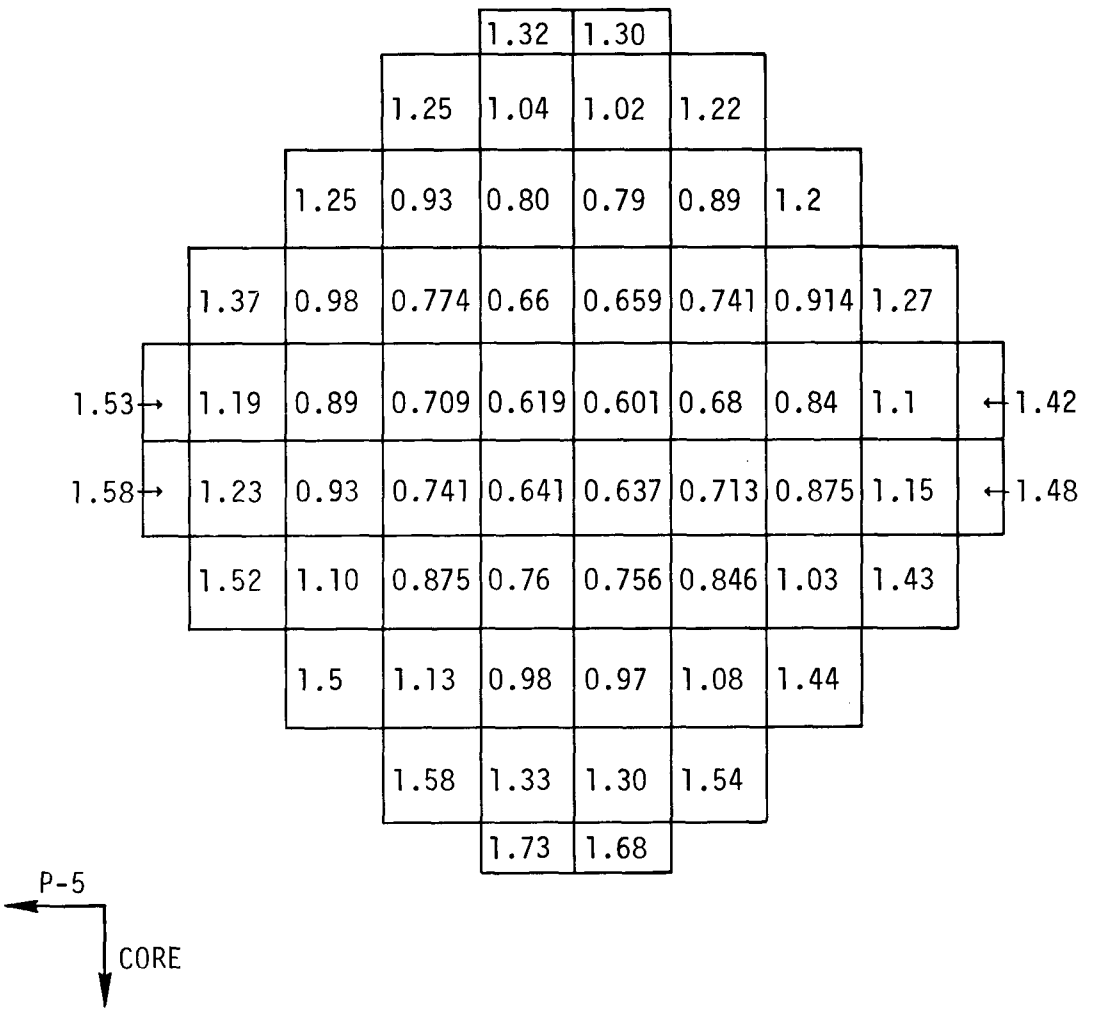

Fig. 4.8. Power distribution within capsule normalized such that $\sum_i P_i V_i = 1.0$

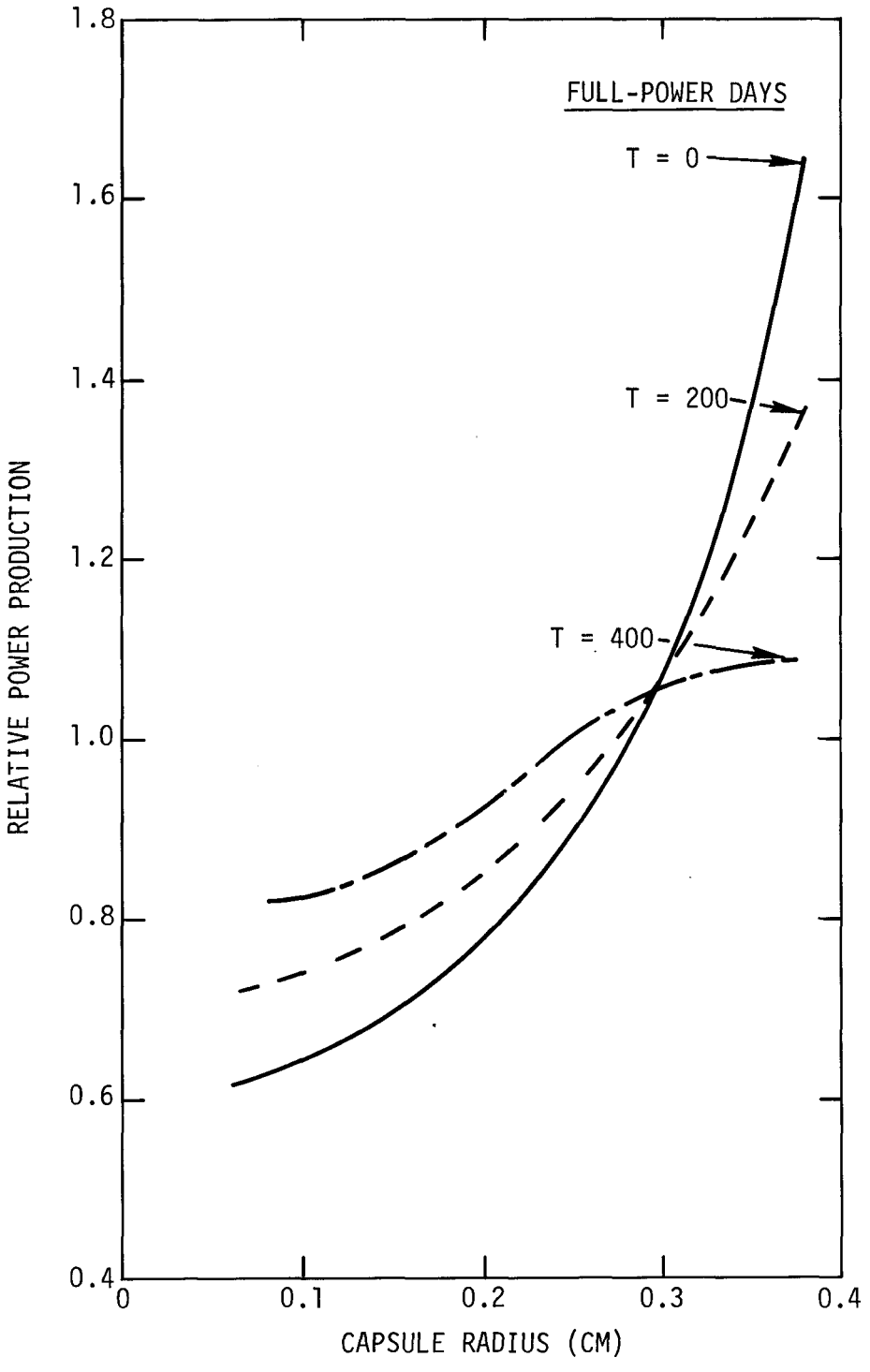

Fig. 4.9. Radial power distribution as a function of burnup in P9 capsule

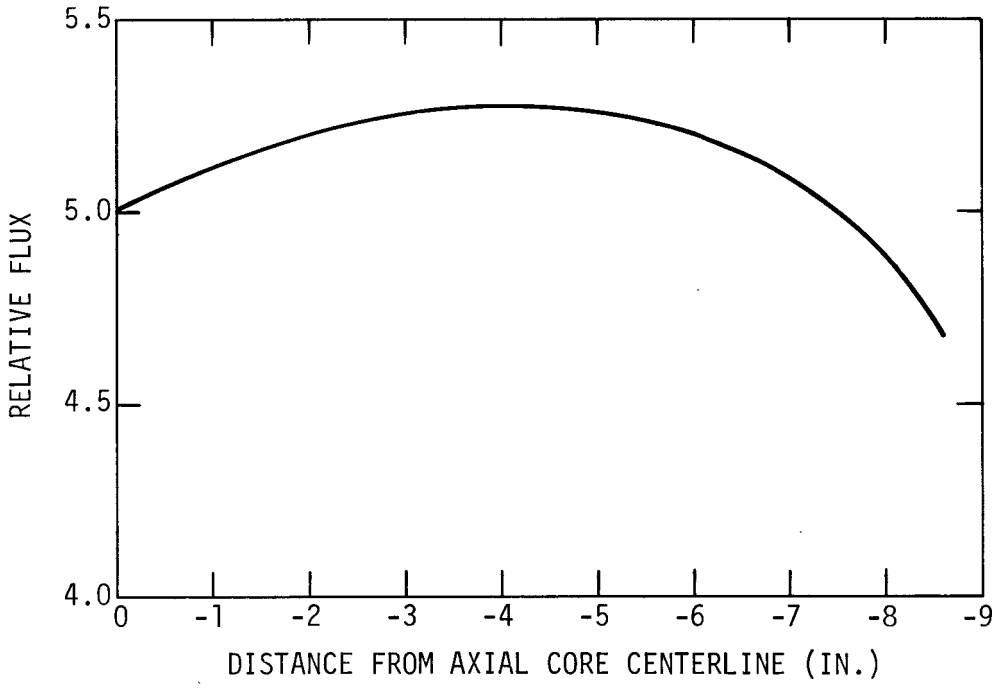

Fig. 4.10. Axial flux shape at position 05

capsule history prior to failure because an uncorrected thermocouple correction factor would tend to overestimate the capsule linear rating.

4.2.3.2. 04-P9 Irradiation Capsule Experimental Studies. Laboratory experiments to determine the diffusion coefficients D_{12} for the krypton-helium gas pair in the P9 capsule mockup have continued during the past quarter. Experimental work has been directed toward determining the nature and cause of the departure of D_{12} from the expected linear dependence on inverse pressure as reported earlier (Ref. 10).

Experiments were undertaken to determine the effect of ion chamber design on the total system. Tests were conducted using a 72-in.-long diffusion tube, in contrast to the previous ∿20-in.-long tube, thus allowing a longer diffusion path. The longer diffusion path should negate any ion chamber volume effects. The test rig was also positioned horizontally to eliminate the possibility of convective flow. Diffusion coefficients were determined at atmospheric pressure and 1000-psi helium pressure using an empty diffusion tube. The computer calculations show essentially the same results for the long and short diffusion tube experiments, thus eliminating the ion chamber volume as a possible experimental artifact.

Additional experiments were conducted using the small diffusion tube at helium pressures of 15, 150, 500, and 1000 psi. The diffusion rig was positioned horizontally and wrapped in silica wool insulation to eliminate convection currents and air drafts in the laboratory. An 8-cm section of the diffusion tube, near the ion chamber, was filled with MI-6736 charcoal to simulate the fuel-rod fission product trap. The experimental data are currently being analyzed using the SLIDER computer program.

4.2.4. Fast Flux Irradiation

Emphasis during this reporting period has been focused on the detailed design analysis for the EBR-II fast flux irradiation of a seven-rod assembly

to determine the technical feasibility of the experiment and permit the submission of the approval-in-principle letter.

The general objective of this test is to study fuel-rod specimens under combinations of conditions that differentiate the GCFR fuel rod from the LMFBR fuel pin, with particular attention to the higher range of cladding temperatures not presently included in the LMFBR program. Variables that will be kept constant are the cladding material (316 stainless steel in the solution-treated condition), the fuel [mixed $(Pu\text{-}U)O_2$], the fuel fabrication technique, and the fuel-rod design. These fixed test conditions are summarized in Table 4.4. Table 4.5 lists the range of temperatures and heat generation rates to be studied, along with the purpose of each set of experimental conditions. The temperature range will overlap that being studied under the LMFBR program to provide a point of commonality for comparison of results; the reference condition selected is the same as that being used in GGA irradiation capsule 04-P9 to provide a direct comparison of fast versus thermal neutron test environment. Interim nondestructive tests are proposed, as well as destructive postirradiation examinations. These tests will study the influence of the test variables on integral rod behavior and individual components.

To obtain the best combination of fluence and burnup, it is advantageous to have a position as close to the center of the core as possible. However, to assess the feasibility of the experiment, the design analysis was performed for a less desirable position, that is, a position in row 7, and it was assumed that at the time of the experiment the reactor would be operating at a power level of 62.5 MW.

As discussed in Refs. 8 and 10, the standard B-7 core subassembly was chosen as a design basis because it uses standard EBR-II hardware and provides space within each capsule for a thermal barrier to increase cladding temperatures. Figure 4.11 illustrates the design of the basic capsule, in which the annular mixed oxide fuel pellet will be surrounded by 316 stainless steel cladding using a helium fuel-cladding bond. Between the cladding and the thermal barrier inner diameter will be a 0.020-in. sodium bond.

TABLE 4.4
FIXED TEST CONDITIONS FOR THE INITIAL SUBASSEMBLY

Cladding	316 SS
Cladding o.d.	0.3 in.
o.d./i.d.	∿1.15
Linear power generation	∿15 kW/ft
Fuel	85 wt-% UO_2 - 15 wt-% PuO_2
Fuel smear density	≤85% TD
External pressure	Ambient
Bond-gap fluid	Helium
Initial internal pressure, hot	40 psig
End-of-life internal pressure, hot	<250 psig

TABLE 4.5
FAST FLUX IRRADIATION CAPSULE LOADINGS

Test Condition		Burnup (MWd/tonne x 1000)				
Temp (deg C)	Heat Generation Rating (kW/ft)	25	50	75	100	Purpose
700	15					Temperature calibration
700	15					Reference/fast flux - thermal flux comparison
700	15					Burnup effect
600	15					Overlap with LMFBR/temperature effect
650	15					Temperature effect
750	15					Temperature effect
800	15					Temperature effect
First Replacement[a]						
700	15					Burnup effect
Second Replacement[b]						
(c)	15					Reproducibility at new reference
(c)	15					Reproducibility at new reference
(c)	15 + x[d]					Influence of higher heat generation rate
(c)	15 - x[d]					Influence of lower heat generation rate
(c)+50	15 + x[d]					Influence of higher temperature plus higher heat generation rate

(a) Does not get benefit of feedback from experiment.
(b) Gets feedback benefit.
(c) New reference temperature, based upon experimental results.
(d) Value of x will be chosen to give reasonable variation from reference heat generation rate.

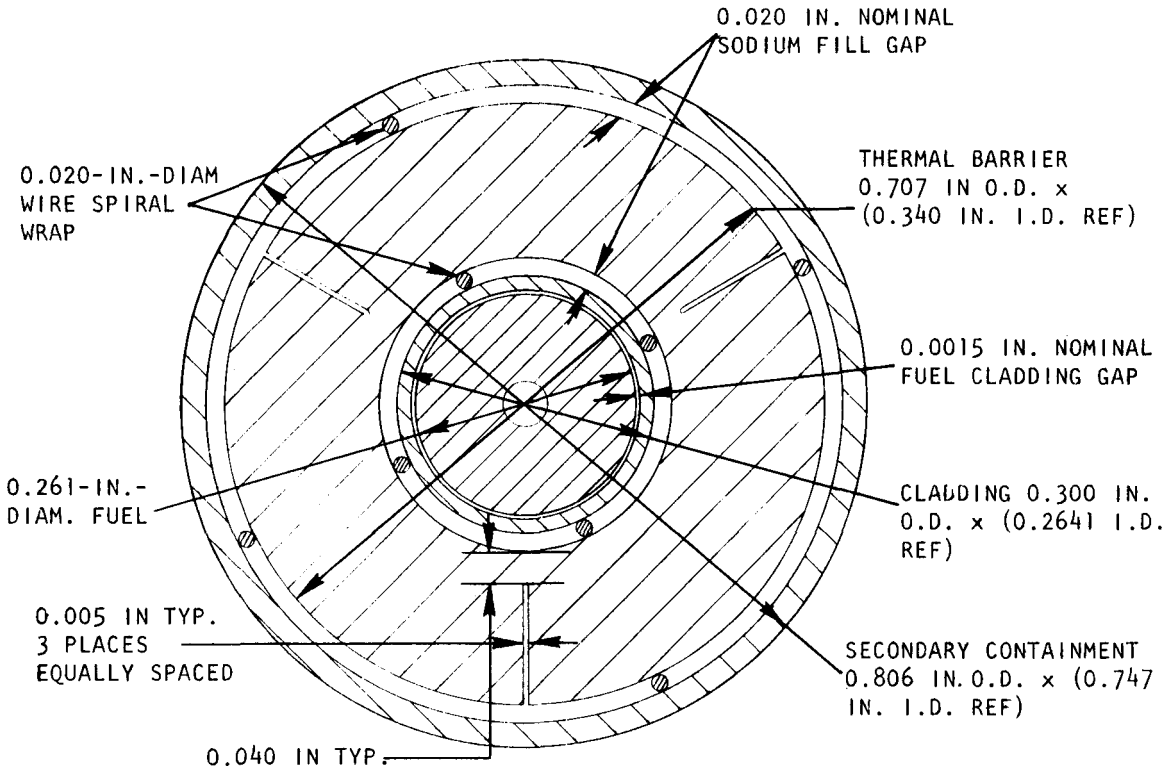

Fig. 4.11. Basic capsule design

The thermal barrier will be a relatively thick tube of 304 stainless steel or Zircaloy with deep radial slots to eliminate thermally induced circumferential stresses. Another sodium bond will be located between the outer diameter of the thermal barrier and the capsule inner diameter.

Analyses of the first subassembly arrangement considered, in which the capsules are allowed to touch each other as shown in Fig. 4.12, have been completed. While the desired peak cladding temperatures of up to 800 C could be realized, the temperature difference between the coolant channels of different shapes was found to be unacceptably large. This situation could be modified by placing an insert in the largest coolant channel to reduce the flow and raise the coolant temperature. However, the use of such an insert is associated with an unacceptably large pressure drop. For these reasons, this design concept was discarded.

In the second configuration considered, shown in Fig. 4.13, a wire wrap is used to separate the capsules. The thermal situation is much better in this design, in which the various coolant channel shapes are more nearly the same in cross-sectional area. If an insert is used in the largest coolant channel, as shown in Fig. 4.14, then a condition can be obtained (S = ∿0.3 in.) for a mean outlet temperature of 425 C where the difference in coolant channel temperatures is only about 42 C, and these conditions are realized with a pressure drop of less than 15 psi.

The reference design selected therefore uses the wire-wrapped capsule and an insert in the largest coolant channel. If a 455 C mean outlet temperature is used as the design value, then some control could be gained later through coolant orificing. Under these conditions, a cladding temperature of 800 C can be realized with a 50 C difference in channel coolant temperatures and a maximum circumferential hot spot of 5 to 10 C greater than the mean temperature.

The cladding temperature of individual fuel rods can be adjusted to give the desired experimental conditions by varying the thickness of the stainless steel thermal barrier. Figure 4.15 illustrates the sensitivity of the

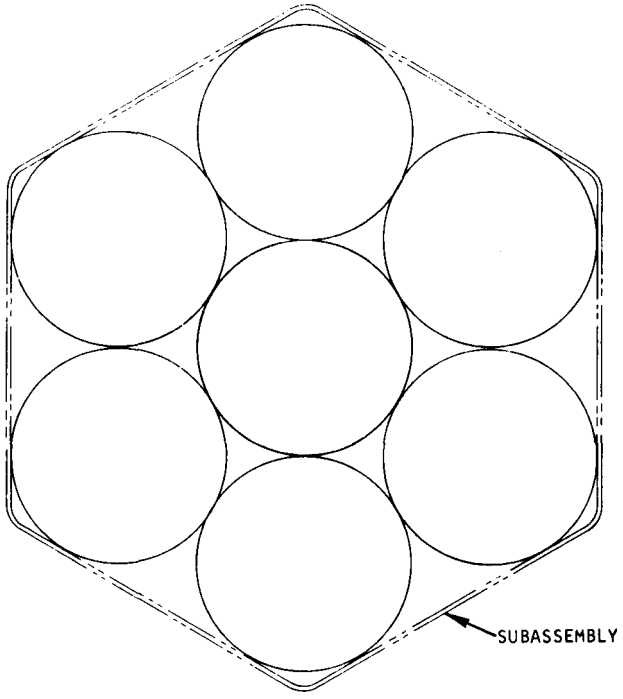

Fig. 4.12. Standard materials irradiation B-7 subassembly design with individual capsules touching

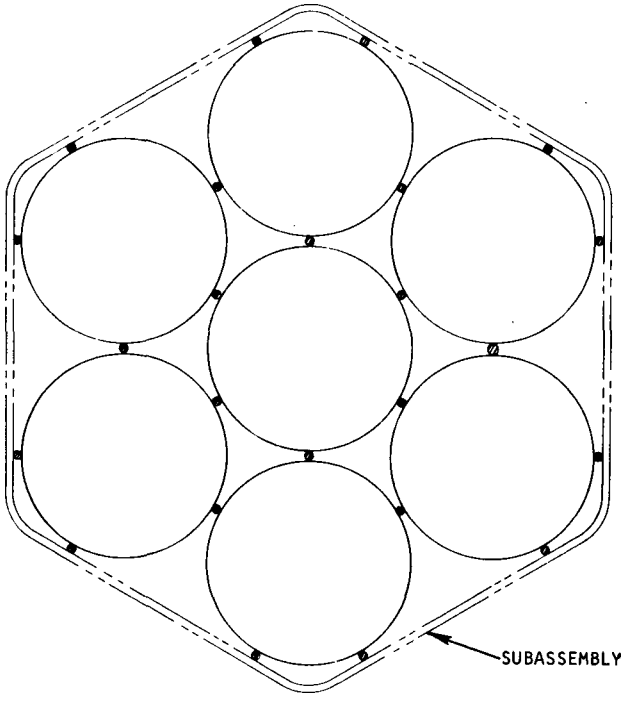

Fig. 4.13. Subassembly design with wire-wrapped capsule configuration

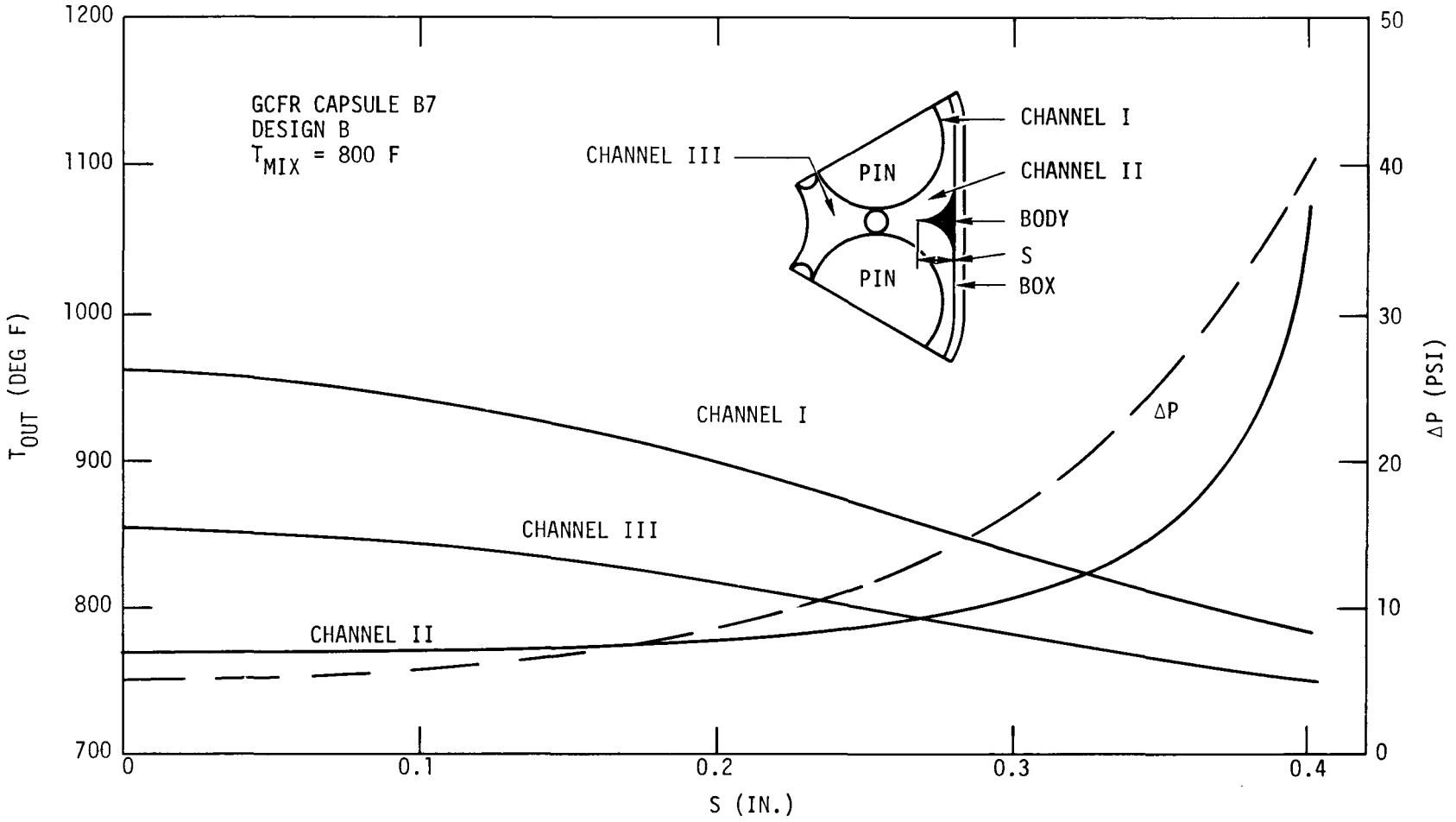

Fig. 4.14. Influence of insert geometry on temperature differences between coolant channels

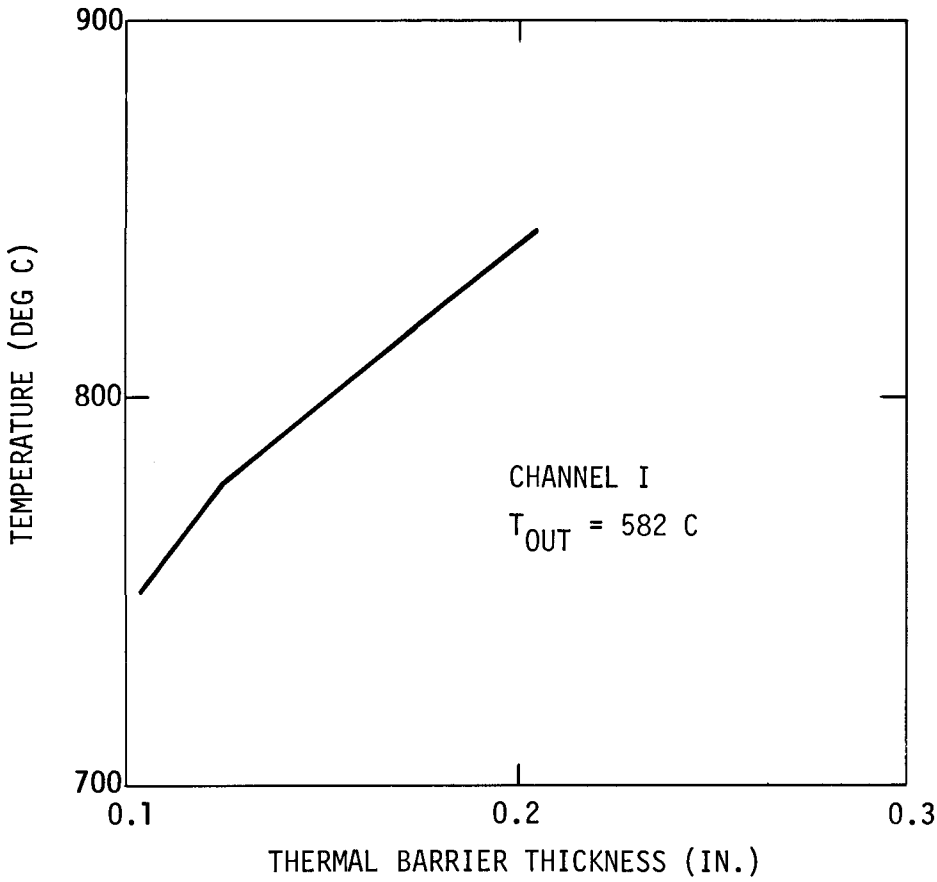

Fig. 4.15. Influence of thermal barrier thickness on cladding temperature

cladding temperature to the thickness of the thermal barrier for the specific case shown.

Additional calculations are being performed to determine the following:

1. Sensitivity of the cladding temperature to

   a. Radial variation in heat transfer coefficient

   b. Uncertainty in neutron flux

   c. Uncertainty in fissile material loading

   d. Flow rate

2. Variations in cladding temperature due to flux variations across a rod and also to flux differences associated with different rod positions within the subassembly

3. The influence of switching the heat barrier material from stainless steel to Zircaloy.

4. The cladding temperature as a function of the thermal barrier thickness for heat generation rates of 12, 15, and 18 kW/ft.

The fluence monitors will be those conventionally used in EBR-II and will utilize the Fe-43(n,p)Mn-54 reaction. For temperature monitoring, which will be more difficult, preliminary selections of techniques have been made. These are the use of SiC rods, which are sensitive to the end-of-irradiation temperature, and measurement of Kr-85 release. Both of these techniques are discussed in Ref. 13.

Using these design parameters as the base, a draft of the approval-in-principle letter has been prepared and is being reviewed prior to submission.

Additional discussions have been held with Atomics International personnel to coordinate efforts such that a common subassembly design would also accommodate their irradiation requirements for carbide fuel rods with heat generation rates of ∿50 kW/ft. A design concept was formulated in which the space envelope for the capsule containing the carbide fuel rods would be the same as that used for the capsules containing the lower heat generation rating oxide fuel rods. To handle the difference in the amount of heat generated, an annular sodium coolant flow channel would be provided within the capsule envelope, and the flow would be adjusted to keep the difference between the inlet and outlet coolant temperatures the same as that obtained in the primary coolant channels surrounding the capsules. Control of the flow in all of the channels would be provided by a variable orificing arrangement. More detailed design and thermal analyses are now being performed to further evaluate the feasibility of this scheme.

REFERENCES

1. "Sodium-Cooled Reactors Fast Ceramic Reactor Development Program, Quarterly Report No. 29, November 1968-January 1969," USAEC Report GEAP-5753, General Electric Co., February 1969.
2. "Sodium-Cooled Reactors Fast Ceramic Reactor Development Program, Quarterly Report No. 27, May-July 1968," USAEC Report GEAP-5677, General Electric Co., August 1968.
3. "Sodium-Cooled Reactors Fast Ceramic Reactor Development Program, Quarterly Report No. 28, August-October 1968," USAEC Report 5700, General Electric Co., November 1968.
4. "Gas-Cooled Fast Breeder Reactor, Quarterly Progress Report for the Quarters August 1, 1967 to July 31, 1968," USAEC Report GA-8787, Gulf General Atomic, September 1968.
5. "Reactor Development Program, Progress Report, August 1969," USAEC Report ANL-7606, Argonne National Laboratory, September 1969.
6. "Reactor Development Program, Progress Report, January 1969," USAEC Report ANL-7548, Argonne National Laboratory, February 1969.
7. Johnson, C. E., and C. E. Croumathal, Argonne National Laboratory, "Cladding Interactions in Mixed Oxide Irradiated Fuels," 1969, unpublished data.
8. "Gas-Cooled Fast Breeder Reactor, Quarterly Progress Report for the Period May 1, 1969 through July 31, 1969," USAEC Report GA-9639, Gulf General Atomic, August 1969.
9. "Gas-Cooled Fast Breeder Reactor, Quarterly Progress Report for the Period August 1 through October 31, 1968," USAEC Report GA-8895, Gulf General Atomic, December 1968.
10. "Gas-Cooled Fast Breeder Reactor, Quarterly Progress Report for the Period February 1, 1969 through April 30, 1969," USAEC Report GA-9359, Gulf General Atomic, June 1969.

11. "Gas-Cooled Fast Breeder Reactor, Annual Progress Report for the Period Ending July 31, 1967," USAEC Report GA-8107, Gulf General Atomic, June 1968.
12. DeCarlo, V. A., et al., "Design of a Capsule for Irradiation Testing of Uranium Nitride Fuel," USAEC Report ORNL-TM-2363, Oak Ridge National Laboratory, February 1969.
13. Bramman, J. I., H. S. Fraser, and W. H. Martin, "Temperature Measurements in Uninstrumented D.F.R. Experiments," International Conference on Fast Reactor Irradiation Testing, April 14-17, 1969, Thurso, Scotland (P/7/7).

5. TASK D - REACTOR PHYSICS PROGRAM

5.1. INTRODUCTION AND SUMMARY

The analysis of the 1-to-1 hydrogen-to-plutonium ratio experiments reported previously (Ref. 1) is essentially complete. Based on this analysis, further experiments are under way and will be completed early in the next quarter. The results of the analysis indicate that the Pu-239 cross-section data set labelled 94.2396 (Ref. 1), which is based on a Karlsruhe evaluation (Ref. 2), gives the best agreement with the critical experiment results over the complete energy range of assemblies considered. Good agreement between analysis and experiment was obtained for the poisoned assemblies; in particular, the new dysprosium cross-section data resulted in far better agreement than the data used in the 5-to-1 hydrogen-to-plutonium ratio assembly analysis (Ref. 3).

5.2. EXPERIMENTAL PROGRAM

An additional set of experiments of interest to the GCFR program has been agreed upon in consultation with PNL personnel. These experiments are now under way and should be completed early in the next quarter.

These experiments will include further checks for the three-dimensional analysis used in this program, the use of an unpoisoned assembly to check leakage effects in the 1-to-1 systems, and an attempt to measure the leakage spectrum from bare and poisoned assemblies with a proton-recoil spectrometer.

The hafnium oxide powder that had been obtained on loan from the American Potash Corporation for use in these experiments was returned at their request.

5.3. ANALYSIS*

In addition to the analysis of the various 1-to-1 hydrogen-to-plutonium ratio critical assemblies, three critical experiments were reevaluated using the current Pu-239 cross-section data of interest. The purpose of this work was to compare the Pu-239 data sets in clean assemblies over a wide range of spectra of interest to the GCFR program. These experiments are the 15-to-1 and 5-to-1 hydrogen-to-plutonium ratio critical assemblies measured at the Hanford Critical Mass Laboratory and the Los Alamos JEZEBEL plutonium metal sphere. When combined with the 1-to-1 experiments, the results of this analysis yield a good integral check on Pu-239 cross-section data over the energy range of interest to the GCFR program. The three Pu-239 evaluated cross-section data sets used in the analysis are summarized in Ref. 1.

The results of this analysis are presented in Table 5.1 and are given in order of decreasing spectral hardness, starting with the JEZEBEL bare plutonium metal sphere. The intercomparison calculations for the 300-MW(e) GCFR Mark I design are also included for completeness.

The results indicate that the 94.2396 Pu-239 data set gives the most satisfactory agreement with the experiments over the energy range of the systems. This data set is based on the Karlsruhe evaluation presented in Ref. 2.

Problems were encountered in the analysis of the 1-to-1 hydrogen-to-plutonium ratio assemblies using one-dimensional transport theory. These difficulties arose because the one-dimensional code was unable to account correctly for leakage from the two zone assemblies, and iterations in the three spatial dimensions for the core multiplication would not converge.

To overcome this difficulty, an analysis using a three-dimensional transport code was performed on the bare unpoisoned assemblies (18-000-003

*The analysis summarized here is being supported by private funds.

TABLE 5.1
SUMMARY OF RESULTS OF INTERCOMPARISON CALCULATIONS FOR VARIOUS HARD-SPECTRUM ASSEMBLIES

System	94.2394 Pu-239 Data		94-2396 Data	94-2398 Data
	k_{eff} Calculation for Actual Assembly	k_{eff} Calculation for Intercomparison System[a]	k_{eff} Calculation for Intercomparison System[a]	k_{eff} Calculation for Intercomparison System[a]
JEZEBEL Pu-metal sphere	1.0141	1.0141	1.0038	0.9822
330 MW(e) GCFR	--	1.0104	1.0179	1.0094
1/1 H/Pu system[b]	1.0058	0.9985	0.9929	0.9735
5/1 H/Pu system[c]	0.9985	1.0094	0.9958	0.9760
15/1 H/Pu system[d]	1.0210	1.0025	1.0107	0.9942

[a] Measured sphere (R = 6.28 cm) used for JEZEBEL intercomparison calculations, and 330 MW(e) Mark I for GCFR calculations. Intercomparison calculations for other systems were performed on sphere with radius chosen to yield $k_{eff} \cong 1.00$ with 94.2394 data.

[b] R = 17.02 cm

[c] R = 19.49 cm

[d] R = 17.89 cm

and 18-000-008) (Ref. 1). Code limitations restricted this analysis to eight energy groups and 15 x 10 x 9 mesh internals. However, the results of the calculations, summarized in Table 5.2, show the distinct improvement in the calculated multiplication factor from this approach.

The other 1-to-1 assemblies could not be analyzed with the three-dimensional transport code due to the limitations in the geometric mockup of the system. However, leakage corrections were obtained from these calculations which yielded good agreement with experiment when used to correct the one-dimensional calculations. The effects of these corrections are also shown in Table 5.2.

The poisoned assemblies were analyzed using 30-group one-dimensional transport calculations including the three-dimensional leakage corrections. The results are summarized in Table 5.3. Results for the corresponding 5-to-1 analysis (Ref. 3) are also included in this table for comparison. The major change is in the dysprosium results, which show a marked improvement in agreement with experiment. This is due to a reevaluation of the resolved resonance parameters for the various dysprosium nuclides, which was suggested by the 5-to-1 results; no other changes were made in the cross-section data.

TABLE 5.2
RESULTS OF ANALYSIS OF 1-TO-1 RATIO CRITICAL ASSEMBLIES

Assembly	Calculated Multiplication Factor, k_{eff}					
	94.2394 Data					
	Original DTF-IV Calc	3DT Calculation	DTF-IV Calc with 3DT Leakage Corr.	94.2394 Data	94.2396 Data	94.2398 Data
18-000-003	1.0358	1.0086	1.0058			
18-000-008		1.0187				
17.02-cm-radius sphere of 1/1 H/Pu fuel for intercomparison calculations				0.9985	0.9929	0.9735

TABLE 5.3
RESULTS OF THE CORRECTED ONE-DIMENSIONAL TRANSPORT ANALYSIS
OF THE 1-TO-1 HYDROGEN-TO-PLUTONIUM RATIO CRITICAL ASSEMBLIES

Assembly	k_{eff} from 1-D Calculation with 3-D Leakage Correction	k_{eff} from 5/1 Analysis
18-000-003	1.0058	
18-000-005 (Dy_2O_3)	1.0095	
18-000-006 (Gd_2O_3)	1.0091	
18-000-007 (HfO_2)	1.0112	
18-000-008	1.0159	
5/1 H/Pu assembly with Dy_2O_3		0.9459
5/1 H/Pu assembly with Gd_2O_3		0.9975
5/1 H/Pu assembly with HfO_2		0.9895

REFERENCES

1. "Gas-Cooled Fast Breeder Reactor, Quarterly Progress Report for the Period May 1, 1969 through July 31, 1969," USAEC Report GA-9639, Gulf General Atomic, August 1969.
2. Langer, I., J. J. Schmidt, and D. Woll, "Tables of Evaluated Neutron Cross Sections for Fast Reactor Materials," KFK-750, Karlsruhe, January 1968.
3. "Gas-Cooled Fast Breeder Reactor, Annual Progress Report for the Period Ending July 31, 1967," USAEC Report GA-8107, Gulf General Atomic, June 1968.